Calorimetric investigations of liquid-crystal compounds exhibiting almost no layer-shrinkage behavior through the smectic-*A*–smectic-*C** transition

K. Ema,* K. Takekoshi, and H. Yao
Department of Physics, Graduate School of Science and Engineering, Tokyo Institute of Technology, 2-12-1 Oh-okayama, Meguro, Tokyo, 152-8550, Japan

S. T. Wang and C. C. Huang
School of Physics and Astronomy, University of Minnesota, Minneapolis, Minnesota 55455, USA
(Received 1 November 2004; published 25 March 2005)

Heat-capacity measurements have been made on liquid-crystal compounds exhibiting almost no layer-shrinkage (NLS) behavior through the Sm-*A*–Sm-*C** phase transition. The transition was found to be second order for two of the substances studied. It was found that the heat-capacity anomaly accompanying a second-order Sm-*A*–Sm-*C** transition with NLS behavior is quite similar to that observed for typical antiferroelectric liquid crystals of the 4-(1-methylheptyloxycarbonyl)phenyl 4′-octyloxybiphenyl-4-carboxylate (MHPOBC) group, showing three-dimensional (3D) *XY* behavior in the vicinity of the transition. On the other hand, for one compound which shows a weakly first-order transition, the anomaly is almost symmetric above and below T_c, with a significant fluctuation effect in the Sm-*A* phase. For this compound, the critical behavior of the heat-capacity anomaly is almost tricritical in the immediate vicinity of T_c, while away from T_c the behavior can be explained with the 3D *XY* model. This suggests that the underlying transition with the 3D *XY* critical behavior is driven to almost being tricritical but remaining weakly first order. No indication of low-dimensional character in the critical behavior was found in both cases.

DOI: 10.1103/PhysRevE.71.031706 PACS number(s): 61.30.Eb, 64.70.−p, 64.60.Fr

I. INTRODUCTION

A class of liquid-crystal compounds has been found which shows almost no layer-shrinkage (NLS) behavior through the Sm-*A*–Sm-*C* (or Sm-*C**) transition. In addition, for chiral materials belonging to this class, unusually large electroclinic effects near the Sm-*A*–Sm-*C** transition have been reported [1–4]. Both a large electroclinic effect and NLS behavior are extremely important in utilizing Sm-*C** material for electro-optical device applications. Thus, a considerable amount of attention has been aimed at understanding the origin of the molecular tilt in the Sm-*C* (or Sm-*C**) phase as well as the true molecular packing arrangement in the Sm-*A* phase of these compounds.

One plausible explanation for these remarkable physical properties is offered by a structure suggested by de Vries *et al.* [5,6]. In this model, the molecules are tilted in the Sm-*A* phase by a finite angle θ_A in the absence of an applied electric field, and are spatially disordered in their azimuths. Specifically, the azimuthal distribution function is uniform, $f(\phi)=1/(2\pi)$, on a cone about the layer normal *z*. Then an applied electric field in the layer plane promotes azimuthal order, without any significant change in θ_A or the smectic layer spacing. A very different theoretical advance based on the idea of a modulated phase has recently been proposed by Meyer and Pelcovits [7].

To be precise, two possible types of structures can be specified in the de Vries model. In the first case [5], the molecules are tilted in a similar way to that in the ordinary Sm-*C* phase, but the tilt directions in different layers are randomly oriented. In the second case [6], the molecules are tilted but there is no long-range order in the tilt direction within each smectic layer. As pointed out by Panarina *et al.* [8], the first possible structure is similar to a unique type of phase called a "sliding phase" [9]. This phase is predicted to occur in weakly coupled three-dimensional (3D) stacks of two-dimensional (2D) *XY* systems. In this respect, the study of critical behavior at the NLS Sm-*A*–Sm-*C* (or *C**) transitions, including clarification of its universality class, is very important.

It has been demonstrated that the high-resolution heat-capacity measurement is a powerful tool in providing us with important information on critical fluctuations. Such an example is the recent heat-capacity measurement carried out by the present authors on 8422[2F3] which shows almost NLS through the Sm-*A*–Sm-*C** transition [10]. That work, referred to as "I" hereafter, revealed a detailed temperature dependence of the heat-capacity anomaly as well as an existence of small latent heat in contrast to an early differential scanning calorimeter (DSC) result [4], and also reported preliminary results of the data analyses [10]. In this paper we describe further detailed analyses of the heat-capacity anomaly for 8422[2F3]. Also included in this paper are high-resolution calorimetric results from two more compounds, 7O23[7F8-] and 8O23[7F8-], displaying NLS behavior. Unusual behavior of surface-induced tilted layers has been observed in free-standing films of 8O23[7F8-] [11]. Figure 1 shows molecular structures and phase sequences of the compounds studied. The values of the transition temperatures in the figure were obtained from DSC measurements carried out at temperature scan rates of about 5 K/min [12].

*Corresponding author. Email address: kema@phys.titech.ac.jp

(a) **8422[2F3]**

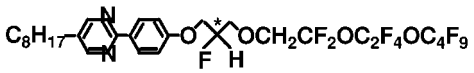

Isotropic (361.5K) SmA (334.7K) SmC*

(b) **7O23[7F8_]**

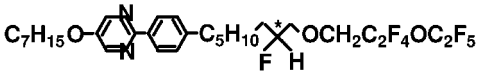

Isotropic (366.3K) SmA (332.7K) SmC*

(c) **8O23[7F8_]**

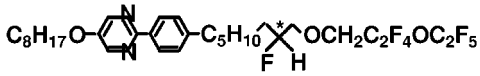

Isotropic (368.7K) SmA (353.1K) SmC*

FIG. 1. Molecular structures and phase sequences of the compounds studied.

II. EXPERIMENTAL DESCRIPTION AND DATA

Heat capacity C_p has been measured with a high-resolution ultralow frequency ac calorimeter [13]. Hermetically sealed gold cells that contained about 20–30 mg of liquid-crystal sample were used. The temperature scan rate was about 0.03 K/h in the transition region. No detectable drift in the Sm-A–Sm-C^* transition temperature was observed, indicating the stability and high quality of the samples.

After subtracting sample cell contributions, typical temperature dependences of C_p data are shown in Fig. 2 for 7O23[7F8-], and Fig. 3 for 8O23[7F8-], respectively. The Sm-A–Sm-C^* transition was observed at 334.2 K in 7O23[7F8-] and 357.4 K in 8O23[7F8-]. The fact that these transition temperatures are higher than the values quoted in Fig. 1 is possibly due to the difference in scan rates. The scan rate used here was about 10^4 times slower than the DSC scan rates. Similar discrepancies were also found for other phase-transition temperatures. In Figs. 2 and 3, the dashed line shows the background heat capacity C_p (background), determined as a quadratic function of temperature which joins the measured heat-capacity data smoothly at temperatures away

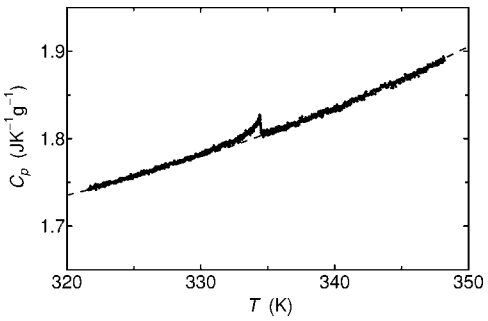

FIG. 2. Temperature dependence of heat capacity from the 7O23[7F8-] sample. The data are acquired in a cooling run. The dashed line shows the background heat-capacity contribution.

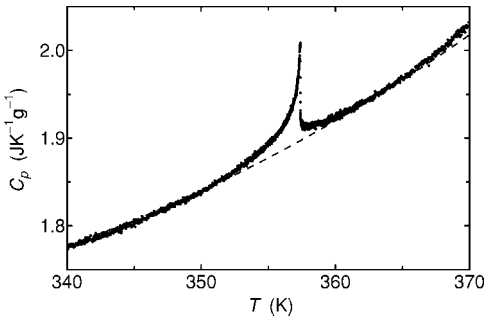

FIG. 3. C_p vs T from the 8O23[7F8-] sample. The data are obtained in a cooling run. The background heat-capacity contribution is shown as the dashed line.

from the transition on both sides of the transition. The increase from the background heat capacity above around 370 K in 8O23[7F8-] is due to a pretransitional behavior approaching the transition to the isotropic phase. In the vicinity of the Sm-A–Sm-C^* transition, the heat capacity displays a distinct λ-shape anomaly for both cases. A nonadiabatic scanning (NAS) mode measurement [14] has also been made, which revealed no indication of the existence of a latent heat for both 7O23[7F8-] and 8O23[7F8-]. Therefore, the transitions are second order for both cases.

In comparison with 7O23[7F8-], the compound 8O23[7F8-] has one additional CH_2 group in the nonchiral alkyl tail. This results in a much smaller Sm-A temperature range for 8O23[7F8-], namely, 16 K for 8O23[7F8-] and 34 K for 7O23[7F8-]. Thus at their respective Sm-A–Sm-C^* transitions, 7O23[7F8-] has a higher order in both nematic and Sm-A order than 8O23[7F8-] does. The observed magnitudes of heat-capacity anomalies for these two compounds are a strong indication of such an effect. Because the anomaly is small, our analyses with a renormalization-group expression as shown below have not been made on 7O23[7F8-].

Excess heat capacity accompanying the transition, denoted as ΔC_p, is obtained by subtracting C_p (background) from the measured C_p data, and is shown in Fig. 4 for 8O23[7F8-]. The temperature dependence of ΔC_p for 8O23[7F8-] is similar to that in 4-(1-methylheptyloxycarbonyl)phenyl 4′-octyloxybiphenyl-4-carboxylate (MHPOBC) and its related antiferroelectric liquid crystals which exhibit the Sm-A–Sm-C_α^* transition [15].

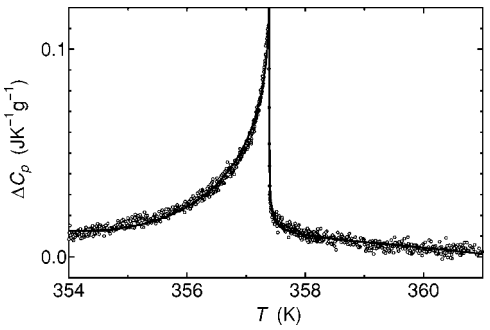

FIG. 4. Temperature dependence of excess heat capacity from the 8O23[7F8-] sample. The solid line is a fit of the data to Eq. (1).

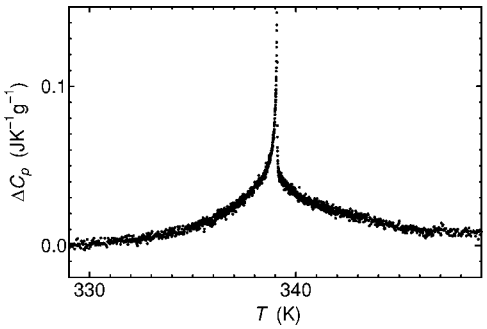

FIG. 5. ΔC_p vs T from the 8422[2F3] sample.

The overall temperature dependence of C_p data for 8422[2F3] has been shown in I. Here, only the ΔC_p data are displayed in Fig. 5. In contrast to the case for 7O- and 8O23[7F8-], the ΔC_p data for 8422[2F3] exhibit a significant feature that the anomaly accompanying the transition is almost symmetric above and below T_c. As reported in I, it was found that the transition in 8422[2F3] is weakly first order, with a small latent heat of about 10 mJ/g, and a narrow two-phase coexistence region of about 16 mK.

III. ANALYSES

The ΔC_p data have been analyzed with the following renormalization-group expression [16]:

$$\Delta C_p = \frac{A^{\pm}}{\alpha}|t|^{-\alpha}(1 + D_1^{\pm}|t|^{\theta} + D_2^{\pm}|t|) + B_c. \quad (1)$$

Here $t=(T-T_c)/T_c$ and the superscripts ± denote above and below T_c. The exponent α was adjusted freely in a least-squares fitting procedure. The correction-to-scaling exponent θ is dependent on the universality class, but has a theoretical value close to 0.5 [16], and therefore was fixed at 0.5 in the first stage of the fitting. There is usually a narrow region in the immediate vicinity of the transition where data are rounded due to impurities and/or instrumental resolutions. The extent of this region was determined in the way described elsewhere [17], and the data inside this region were excluded in the fitting. In the present fits, the rounding region thus determined is $-8.1\times10^{-5}<t<+0.3\times10^{-5}$ for 8O23[7F8-], and $-8.0\times10^{-5}<t<+1.2\times10^{-5}$ for 8422[2F3].

A. Analyses on 8O23[7F8-]

The parameter values obtained in fitting the ΔC_p data for 8O23[7F8-] are shown in Table I. Fits were made to the data over several ranges, and the maximum value of $|t|$ used in the fit, denoted as $|t|_{\max}$, is included in the table. When the exponent α has been adjusted freely (fits 1-3), its value is close to zero for small $|t|_{\max}$, and becomes larger for wider fitting ranges. Such a feature is the same as those being observed in the MHPOBC-group antiferroelectric liquid crystals [15]. In Table I, fits 4-7 show the results when the exponents have been fixed at the 3D-XY theoretical values, $\alpha_{XY}=-0.0066$ and $\theta_{XY}=0.524$ [16]. The quality of the fit is adequate for $|t|_{\max}=0.001$. Inclusion of the second-order correction terms yields satisfactory fits for wider fitting ranges in the χ_ν^2 sense. As an example, the result for fit 7 is shown as the solid line in Fig. 4. It is noticed, however, that violation of the scaling prediction $D_1^-/D_1^+>0$ is seen in all cases. This feature is again similar to the case of the MHPOBC-group substances [15]. Thus we can conclude that the ΔC_p data in 8O23[7F8-] show 3D XY critical behavior near T_c, which crosses over to tricritical behavior just as in antiferroelectric liquid crystals of the MHPOBC group. The critical amplitude ratio A^-/A^+ for 8O23[7F8-] has a value of 0.90–0.96 depending on the fitting condition. If we take as the most reliable value the one with $|t|_{\max}=0.001$, we have the value $A^-/A^+=0.901$, which is slightly smaller than the theoretical value 0.971, and also smaller than corresponding values around 0.96 for MHPOBC, MHPBC, and 12BIMF10, and 0.922 for MHPOCBC [15].

B. Analyses on 8422[2F3]

As reported already in I, the transition is weakly first order in 8422[2F3]. Nevertheless, because the first-order nature of the transition is very weak, the use of Eq. (1) for the analysis is justified as a starting trial function.

The results of the fitting are summarized in Table II as fits 1-3. For $|t|_{\max}=0.001$ and 0.003, the α value is close to the tricritical value 0.5. This seems reasonable because the transition is very weakly first order and therefore close to a tricritical point which corresponds to a border between second- and first-order transitions. It is also seen that $D_1^{\pm}$ values are anomalously large. Because the transition is first order, the critical constant term B_c need not be equal above and below T_c, implying an existence of a gap $\Delta B_c \equiv B_c^+ - B_c^-$ at T_c. When

TABLE I. Fitting parameters and least-squares values obtained from fittings of the 8O23[7F8-] ΔC_p data to Eq. (1). The quantities in the brackets have been fixed at the values shown in the table. The units are JK^{-1} g^{-1} for A^+ and B_c, and K for T_c.

fit	$\lvert t\rvert_{\max}$	T_c	α	θ	10^3A^+	A^-/A^+	D_1^+	D_1^-	D_2^+	D_2^-	B_c	χ_ν^2
1	0.001	357.393	0.043	[0.5]	3.904	1.769	1.88	−6.78	[0]	[0]	−0.115	1.00
2	0.003	357.393	0.152	[0.5]	0.946	4.891	−6.40	−10.63	[0]	[0]	−0.001	1.10
3	0.01	357.393	0.237	[0.5]	0.3527	8.535	−35.44	−11.69	[0]	[0]	0.014	1.39
4	0.001	357.393	[−0.0066]	[0.524]	7.258	0.901	−0.42	2.12	[0]	[0]	1.053	1.10
5	0.003	[357.393]	[−0.0066]	[0.524]	8.941	0.931	−0.30	0.95	[0]	[0]	1.296	2.81
6	0.01	[357.393]	[−0.0066]	[0.524]	12.111	0.961	−0.20	0.27	[0]	[0]	1.755	6.97
7	0.01	[357.393]	[−0.0066]	[0.524]	8.314	0.919	−0.41	1.72	2.2	−9.2	1.205	1.58

TABLE II. Adjustable parameters and least-squares values acquired from fittings of the 8422[2F3] ΔC_p data to Eq. (1) or Eq. (2). The quantities in the brackets have been fixed at the values shown in the table. The units are $JK^{-1}g^{-1}$ for A^+, B_c, and ΔB_c, and K for T_c.

Fit	$\lvert t\rvert_{\max}$	T_c	α	θ	10^5A^+	A^-/A^+	D_1^+	D_1^-	D_2^+	D_2^-	B_c	ΔB_c	χ_ν^2
1	0.001	339.103	0.550	[0.5]	1.680	20.88	1189	46	[0]	[0]	−0.014	[0]	1.00
2	0.003	339.104	0.525	[0.5]	0.740	56.1	9993	166	[0]	[0]	−0.130	[0]	1.11
3	0.01	339.084	0.328	[0.5]	11.296	9.93	−323	−44.7	[0]	[0]	0.069	[0]	1.74
4	0.001	339.101	0.472	[0.5]	8.677	7.926	[0]	[0]	[0]	[0]	0.035	0.017	1.04
5	0.003	[339.101]	0.385	[0.5]	22.559	6.132	[0]	[0]	[0]	[0]	0.029	0.025	1.42
6	0.01	[339.101]	0.167	[0.5]	201.23	3.427	[0]	[0]	[0]	[0]	−0.002	0.071	3.61
7	0.01	[339.101]	0.599	[0.5]	1.552	13.165	[0]	[0]	−7095	−770	0.048	−0.003	1.25

$\alpha \sim 0.5$ and $\theta \sim 0.5$, the first-order correction term, with a temperature dependence $|t|^{\theta-\alpha}$ behaves almost as a constant term, and tends to account for the gap by adjusting $D_1^\pm$ values.

Before describing further results, we note a point related to the first-order nature of the transition which might affect our analyses. At first-order transitions, the temperature where ΔC_p diverges will be different when the transition is approached from above or below the transition temperature. This can be taken into account by replacing the reduced temperature t by $t \equiv (T - T_c^\pm)/T_c^\pm$, where superscripts ± denote above and below T_c. It is expected that T_c^+ is lower than T_c^-, thus $\Delta T_c \equiv T_c^- - T_c^+$ should be positive. It was found, however, that the quality of the fit became slightly worse with increasing ΔT_c from zero. This indicates that first-order nature of the transition is quite weak in the present case so that we can practically assume $\Delta T_c = 0$.

As the next stage of our analyses, we fitted the data with the following expression:

$$\Delta C_p = \frac{A^\pm}{\alpha}|t|^{-\alpha}(1 + D_2^\pm|t|) + B_c^\pm. \tag{2}$$

The difference between Eqs. (1) and (2) is that the first-order correction term has been merged into the critical constant term B_c's which can differ for above and below T_c. The results are shown as fits 4-7 in Table II. Allowing nonzero D_2's for $|t|_{\max} = 0.01$ improves the quality of the fitting in χ_ν^2 sense, with artificially large D_2 values. This implies that Eq. (2) does not describe the anomaly adequately. In other words, the deviations from the asymptotic critical behavior away from T_c are not explained as corrections to the scaling, but rather a manifestation of an essentially different critical behavior. Further analyses will be described below in connection with the results on H8F(4,2,1)MOPP reported by Iannacchione *et al.* [18].

IV. DISCUSSION

Quite interestingly, we see that behaviors of heat-capacity anomalies at the Sm-A–Sm-C^* transition reported in this paper can be classified into two types: one is that of 7O23[7F8-] and 8O23[7F8-], the other is that of 8422[2F3]. This might be related to the order of the transition. Most of the NLS compounds studied so far, such as 8422[2F3], show first-order Sm-A–Sm-C^* transitions. Although the transition in TSiKN65 was reported to be second order in an earlier study [8], recent measurements made by some of the present authors have revealed that it is weakly first order [19]. On the other hand, results presented here reveal that the Sm-A–Sm-C^* transitions in 7O23[7F8-] and 8O23[7F8-] are second order. It deserves attention that the fluctuation effect is more significant in the case of a first-order transition. For 8422[2F3] the C_p anomaly in the Sm-A phase is almost as large as that in the Sm-C^* phase. At $T = T_c + 0.5$ K, we have $\Delta C_p \sim 0.036$ J/gK, which can be compared with the corresponding value of 0.026 J/gK for MHPOBC. In 8O23[7F8-], on the other hand, the fluctuation anomaly in the Sm-A is visible but definitely smaller than in the Sm-C^* phase. At $T = T_c + 0.5$ K, we have $\Delta C_p \sim 0.012$ J/gK for this case. We note that the transition is very close to the tricritical one not only in 8422[2F3] as described here, but also in TSiKN65 [19], suggesting that the transition can be driven to first order by some mechanisms. It is known that fluctuations drive some phase transitions to first order. For the ordinary Sm-A–Sm-C transitions, it is expected that the transition becomes first order due to several factors including the width of Sm-A phase range [20]. In case of the nematic(N)–Sm-A transition, it is driven to first order through the coupling between the nematic and smectic order when the nematic order is small and its fluctuation becomes important [21]. It was found that the nematic order is 0.56 [4,22] in case of 8422[2F3], which is about 25% lower than the typical value 0.7–0.8 in ordinary Sm-A phases. We can expect that such low nematic order allows much more room for fluctuations, and the coupling to the smectic order becomes important. As another information on this line, on the other hand, an apparent distinction is found in the values of the layer thickness difference for the Sm-A and Sm-C^* phases, being about 0.7% for 8422[2F3] [10], and 1.2% for 8O23[7F8-] [23]. This suggests that the mechanism of NLS behavior is less effective in 8O23[7F8-]. In any case, more detailed precise information as to the behavior of the nematic order around the transition is needed.

Another interesting comparison can be made with H8F(4,2,1)MOPP studied by Iannacchione *et al.* [18]. This compound has a chemical structure quite similar to 8422[2F3], and exhibits NLS behavior through the achiral Sm-A–Sm-C transition [24]. It was reported that this compound shows very strong energy fluctuations in the Sm-A

TABLE III. Fitting parameters and least-squares values obtained from fittings of the 8422[2F3] ΔC_p data to Eq. (1). The quantities in the brackets have been fixed at the values shown in the table. The units are $JK^{-1}g^{-1}$ for A^+ and B_c, and K for T_c.

Fit	$\|t\|_{max}$	$\|t\|_{min}$	T_c	α	θ	10^3A^+	A^-/A^+	D_1^+	D_1^-	B_c	χ_ν^2
1	0.02	0.003	338.443	[−0.0066]	[0.524]	14.675	1.005	[0]	[0]	2.179	1.20
2	0.03	0.003	338.479	[−0.0066]	[0.524]	14.181	1.004	[0]	[0]	2.106	1.32
3	0.02	0.003	338.290	[−0.0066]	[0.524]	15.847	1.006	−0.004	−0.020	2.351	1.19
4	0.03	0.003	338.232	[−0.0066]	[0.524]	18.035	1.006	−0.017	−0.039	2.670	1.22

phase. At $T=T_c+0.5$ K, $\Delta C_p \sim 0.15$ J/gK is read from Fig. 2 in Ref. [18], much larger than the values mentioned above. They also found that the ΔC_p data can be well described by the 3D *XY* model over a wide temperature range up to $|t|_{max} \sim 0.03$. To compare the present results with this, we tried fitting the present data on 8422[2F3] over a wider range. In these fits, the data close to T_c, with $|t|<|t|_{min}=0.003$ have been omitted to exclude critical behavior in the vicinity of T_c, and to evaluate the behaviors of the heat-capacity anomaly in the range away from T_c. [In case of H8F(4,2,1)MOPP, data in a range $-0.000\,16<t<+0.003$ had to be excluded in fitting due to history-dependent anomalous C_p behavior ascribed to impurity effect.] The exponents have been fixed at the 3D *XY* values: $\alpha=-0.0066$ and $\theta=0.524$ [16]. The obtained parameter values are shown in Table III. The D_1 values are rather small, being on the order of 0.01, and satisfy the scaling prediction $D_1^+/D_1^->0$. The critical amplitude ratio is $A^-/A^+ \sim 1.005$, presenting a quite unusual example since it exceeds unity. This value is in disagreement with the theoretical value of 0.971 for 3D *XY*, while it is closer to 1.029 for the *inverted XY* model. We also note the value from H8F(4,2,1)MOPP, 0.994-0.995, although slightly less than unity, almost agrees with the present value for 8422[2F3]. As a whole, the behavior of the heat-capacity anomaly in the range away from T_c can also be explained by the 3D *XY* model.

In conclusion, the high-resolution calorimetric measurements presented here, have revealed two types of heat-capacity anomalies which considerably differ from each other: the one in 7O- and 8O23[7F8-], and the other in 8422[2F3]. The transition is second order in the former while it is weakly first order in the latter. Fluctuation effects are more significant in the latter case. In addition, the extent of the NLS behavior seems larger in the latter. These facts suggest that the difference is due to the magnitude of the mechanism causing the NLS behavior. On the other hand, both cases can be classified into the same universality class of 3D *XY*, without showing any indication of low-dimensional character expected in the "sliding phase." In the de Vries picture the local tilt does not show a noticeable anomaly at T_c, so that the order parameter has a two-dimensional degree of freedom, the position and magnitude of angular distribution function, and therefore justifies the *XY* nature of the transition. It may be worthy to note that this situation is similar to the N–Sm-*A* transition. In the N–Sm-*A* transition, modulation in the density function along the *z* axis results in the smectic order. In the de Vries picture, modulation in the azimuthal distribution function is responsible for the transition. In any case, the apparent *inverted XY* behavior has to be verified from a theoretical viewpoint.

At present, experimental data on the Sm-*A*–Sm-*C* (or Sm-C^*) transitions with NLS behavior are limited both in quantitative and qualitative sense. Further high-resolution experiments as well as theoretical investigations are urgently needed.

ACKNOWLEDGMENTS

The authors are grateful to Dr. A. Cady for critical reading of the manuscript. This work was partially supported by the National Science Foundation, Solid State Chemistry, under Grant No. DMR-0106122, and the Donor of the Petroleum Research Fund, administered by the American Chemical Society. The liquid-crystal compounds were kindly provided by 3M Company, St. Paul, Minnesota.

[1] M. S. Spector, P. A. Heiney, J. Naciri, B. T. Weslowski, D. B. Holt, and R. Shashidhar, Phys. Rev. E **61**, 1579 (2000).
[2] J. V. Selinger, P. J. Collings, and R. Shashidhar, Phys. Rev. E **64**, 061705 (2001).
[3] N. A. Clark, T. Bellini, R. F. Shao, D. Coleman, S. Bardon, D. R. Link, J. E. Maclennan, X. H. Chen, M. D. Wand, D. M. Walba, P. Rudquist, and S. T. Lagerwall, Appl. Phys. Lett. **80**, 4097 (2002).
[4] J. P. F. Lagerwall, F. Giesselmann, and M. D. Radcliffe, Phys. Rev. E **66**, 031703 (2002).
[5] A. de Vries, Mol. Cryst. Liq. Cryst. **41**, 27 (1977).
[6] A. de Vries, A. Ekachai, and N. Spielberg, Mol. Cryst. Liq. Cryst. **49** (L), 143 (1979); A. de Vries, *ibid.* **49** (L), 179 (1979).
[7] R. B. Meyer and R. A. Pelcovits, Phys. Rev. E **65**, 061704 (2002).
[8] O. E. Panarina, Yu. P. Panarin, J. K. Vij, M. S. Spector, and R. Shashidhar, Phys. Rev. E **67**, 051709 (2003).
[9] C. S. O'Hern, T. C. Lubensky, and J. Toner, Phys. Rev. Lett. **83**, 2745 (1999).
[10] C. C. Huang, S. T. Wang, X. F. Han, A. Cady, R. Pindak, W. Caliebe, K. Ema, K. Takekoshi, and H. Yao, Phys. Rev. E **69**, 041702 (2004).
[11] S. T. Wang, X. F. Han, Z. Q. Liu, A. Cady, M. D. Radcliffe,

and C. C. Huang, Phys. Rev. E **68**, 060702 (2003).
[12] The transition temperatures were provided by Dr. M. D. Radcliffe at 3M Company.
[13] K. Ema and H. Yao, Thermochim. Acta **304/305**, 157 (1997).
[14] H. Yao, K. Ema, and C. W. Garland, Rev. Sci. Instrum. **69**, 172 (1998).
[15] K. Ema and H. Yao, Phys. Rev. E **57**, 6677 (1998).
[16] C. Bagnuls and C. Bervillier, Phys. Rev. B **32**, 7209 (1985).
[17] H. Haga, A. Onodera, Y. Shiozaki, K. Ema, and H. Sakata, J. Phys. Soc. Jpn. **64**, 822 (1995).
[18] G. S. Iannacchione, C. W. Garland, P. M. Johnson, and C. C. Huang, Liq. Cryst. **26**, 51 (1999).
[19] (Unpublished).
[20] S. C. Lien and C. C. Huang, Phys. Rev. A **30**, 624 (1984); Ch. Bahr and G. Heppke, Phys. Rev. Lett. **65**, 3297 (1990).
[21] W. L. McMillan, Phys. Rev. A **4**, 1238 (1971); K. Kobayashi, J. Phys. Soc. Jpn. **29**, 101 (1970); P. G. de Gennes, Solid State Commun. **10**, 753 (1972), Mol. Cryst. Liq. Cryst. **21**, 49 (1973).
[22] The magnitude of the nematic order was determined by fitting to the wide-angle x-ray scattering data from bulk aligned samples.
[23] S. T. Wang, Z. Q. Liu, R. Pindak, W. Caliebe, and C. C. Huang (unpublished).
[24] P. Mach, P. M. Johnson, E. D. Wedell, F. Lintgen, and C. C. Huang, Europhys. Lett. **40**, 399 (1997).